11-2005

Observation of Large Photoacoustic Signal Phase Changes During a Diffusion Process

Stanley J. Bajic
Iowa State University, sjbajic@ameslab.gov

Roger W. Jones
Iowa State University, jonesrw@ameslab.gov

John F. McClelland
Iowa State University, mcclelland@ameslab.gov

Observation of Large Photoacoustic Signal Phase Changes During a Diffusion Process

Abstract

The phase of the photoacoustic signal is known to be a sensitive and accurate means to investigate, both qualitatively and quantitatively, static multilayer heterogeneous systems. According to theory, the maximum phase delay for a very weakly absorbing homogeneous sample should be within 45° of a very strongly absorbing sample, while for heterogeneous samples the phase delay can be greater than 45°. Here we report the observation of photoacoustic phase delays *greater than 350*° by extending the use of step-scan phase modulation photoacoustic spectroscopy to study a non-repetitive dynamic system *in situ,* in real time. These large phase delays correspond to sampling several thermal diffusion lengths into the sample. The model system used in this study consisted of a hydrocarbon grease diffusing through a porous Teflon film. The progress of the diffusion was tracked by monitoring both the photoacoustic signal magnitude and the phase of the hydrocarbon grease after isolation from the Teflon film signal contributions at two different phase modulation frequencies.

Keywords

Biochemistry Biophysics and Molecular Biology, Mechanical Engineering, Depth profiling, diffusion monitoring, phase-resolved profiling by PAS, photoacoustic spectroscopy

Disciplines

Acoustics, Dynamics, and Controls | Biochemistry, Biophysics, and Structural Biology | Mechanical Engineering

Comments

This paper was published in *Applied Spectroscopy* 59 (2005): 1420 and is made available as an electronic reprint with the permission of OSA. The paper can be found at the following URL on the OSA website: doi: 10.1366/000370205774783142.

Observation of Large Photoacoustic Signal Phase Changes During a Diffusion Process

STANLEY J. BAJIC,* ROGER W. JONES, and JOHN F. McCLELLAND

Ames Laboratory, Iowa State University, Ames, Iowa 50011 (S.J.B., R.W.J., J.F.M.); and MTEC Photoacoustics, Inc., P.O. Box 1095, Ames, Iowa 50014 (J.F.M.)

The phase of the photoacoustic signal is known to be a sensitive and accurate means to investigate, both qualitatively and quantitatively, static multilayer heterogeneous systems. According to theory, the maximum phase delay for a very weakly absorbing homogeneous sample should be within 45° of a very strongly absorbing sample, while for heterogeneous samples the phase delay can be greater than 45°. Here we report the observation of photoacoustic phase delays *greater than 350°* by extending the use of step-scan phase modulation photoacoustic spectroscopy to study a non-repetitive dynamic system *in situ,* in real time. These large phase delays correspond to sampling several thermal diffusion lengths into the sample. The model system used in this study consisted of a hydrocarbon grease diffusing through a porous Teflon film. The progress of the diffusion was tracked by monitoring both the photoacoustic signal magnitude and the phase of the hydrocarbon grease after isolation from the Teflon film signal contributions at two different phase modulation frequencies.

Index Headings: **Photoacoustic spectroscopy; Diffusion monitoring; Depth profiling; Phase-resolved profiling by PAS.**

INTRODUCTION

It is well known that photoacoustic spectroscopy, which is based on the optoacoustic effect discovered by Alexander Graham Bell,[1] can be used to obtain sample depth information from static layered samples or samples that contain gradients.[2–14] In this work, we have extended the use of photoacoustic spectroscopy as a novel means of studying a non-repetitive dynamic system. The system studied consisted of a hydrocarbon grease diffusing through a porous Teflon film. Both the phase and magnitude at two different phase modulation frequencies were used to monitor the diffusion of the grease through the Teflon film. Photoacoustic signal contributions from the Teflon film and the sample chamber background were subtracted from the total phase and magnitude in order to isolate the grease signal. Large phase shifts (*greater than 350°*) were observed for the isolated grease signal over the course of diffusion, corresponding to sampling of several diffusion lengths into the sample.

From Rosencwaig and Gersho,[15] the sampling depth, which is taken to be the thermal diffusion length, L, for a homogeneous material is approximated by

$$L = \left(\frac{D}{\pi f}\right)^{1/2} \tag{1}$$

where D is the thermal diffusivity and f is the modulation frequency. This approximation assumes that light penetration exceeds L. Otherwise the sampling depth is determined by $1/\alpha$, where α is the sample absorption coefficient. In conventional rapid-scan Fourier transform infrared (FT-IR) spectrometry, L varies across the spectrum because of the wavenumber dependence of the modulation frequency (i.e., $f = v\bar{\nu}$ where $\bar{\nu}$ is the infrared wavenumber and v is the scanning velocity). When one uses a step-scan FT-IR spectrometer with phase modulation, the wavenumber dependence is removed, consequently producing a uniform modulation frequency (and hence sampling depth) across the infrared spectrum. Accordingly, by acquiring data at several different phase modulation frequencies one can obtain information at several different sampling depths.

Step-scan FT-IR spectrometers typically use analog demodulation or digital signal processing (DSP) to deconvolve the photoacoustic signal into its magnitude and phase components. The phase signal varies according to the depth at which components are distributed, since it is directly related to the time required for heat generated at a particular depth by absorption to be transported to the surface of the sample. Several authors have previously covered depth profiling using step-scan phase modulation photoacoustic spectroscopy in greater detail.[3,7–9,13,16–18] The reader is referred to these.

The permeation or diffusion of organic materials through polymer films has been an active area of interest in a number of different areas: drug delivery, polymer degradation, environmental sensors, and food packaging safety. A number of different analytical techniques have been used to study various diffusion systems (e.g., attenuated total reflection (ATR),[19–22] nuclear magnetic resonance (NMR),[23] ultraviolet–visible,[24] X-ray fluorescence (XRF),[25] and fluorescence[26]). These techniques, however, usually require that the diffusion be stopped before spectroscopic interrogation, so the process must be repeated for a set of time periods to build up a set of observations. In this paper, we describe using step-scan phase modulation photoacoustic spectroscopy as a novel method of observing a diffusion front moving through a matrix in real time.

EXPERIMENTAL

All data were collected on a BioRad Digilab FTS-60A FT-IR spectrometer equipped with a BioRad demodulator and a helium purged MTEC Model 200 photoacoustic cell. The spectrometer was controlled and all data manipulated with Win-IR Pro software. Phase modulation data were collected in the multichannel spectroscopy (MCS) mode at modulation frequencies of 400 Hz and 25 Hz at a laser fringe amplitude of 2 and with scanning velocities of 25 Hz and 2.5 Hz, respectively. A low res-

Received 10 June 2005; accepted 2 September 2005.

* Author to whom correspondence should be sent.

0003-7028/05/5911-1420$2.00/0

olution of 32 cm^{-1} was used to reduce the number of points needed during a scan, thereby reducing the acquisition time per scan. Eight scans were coadded for the 400 Hz phase-modulation data (requiring 3 min 30 s), while only a single scan was used for the 25 Hz phase-modulation acquisition (3 min 45 s). All magnitude spectra were normalized against 60% carbon-black-filled rubber to account for spectral variations due to the infrared source and spectrometer.[27]

The penetrant used was Apiezon-L Grease (Apiezon Products, U.K.), which is a low vapor pressure petrolatum hydrocarbon grease containing no additives. A special sample cup was prepared that had a deep cavity, which was filled with the Apiezon-L grease, and a large brim to support the Teflon film. The deep cavity allowed for an effectively infinite supply of grease, thereby assuring that the process was not penetrant limited. A suitably sized piece of Teflon film was cut from a roll and placed directly over the cup and grease. A ring was then placed over the Teflon to eliminate any signal generation from the edges of the film or the underlying grease. The sample was then immediately placed into the detector and data taken, alternating between 400 Hz and 25 Hz phase-modulation acquisitions.

The Teflon film used in this experiment consisted of an unsintered extruded porous film (Garlock Sealing Technologies, Inc., Palmyra, NY) that had a thickness of approximately 254 μm. The film, which comprised a network of fibrils and particles, had a density of approximately 1.5 g/cm^3, versus 2.2 g/cm^3 for solid Teflon, resulting in an approximately 32% pore volume. The pore structure of the film was of submicrometer dimensions. The film was washed in hexane and oven dried to remove any hydrocarbons present prior to use.

The thermal diffusivity of the porous Teflon film is unknown, so the calculated thermal diffusivity of solid Teflon, $D_{\text{Teflon(solid)}} \approx 1.09 \times 10^{-3}$ cm^2/s, was used.[28] The thermal diffusivity of Apiezon-L grease is $D_{\text{Apiezon-L}} \approx 1.2 \times 10^{-3}$ cm^2/s.† Based on the thermal diffusivity of solid Teflon the thermal diffusion lengths for 400 Hz and 25 Hz modulation frequencies were determined to be 9.5 μm and 36 μm, respectively.

To confirm the stability of the cell response over the length of time of the diffusion, a helium leak test was performed. The test was performed by monitoring the change in magnitude of the photoacoustic signal from a carbon black reference sample over a period of time. A helium atmosphere is desired in the sample chamber because it produces a larger photoacoustic signal than air. The test showed that the magnitude changed less than 2% over six hours. A larger change in the magnitude would indicate leaking of air into the photoacoustic chamber affecting reproducibility and stability of the measurements.

Data Processing. Collecting data in the MCS mode yields in-phase and quadrature interferograms, at 0° and 90°, respectively, which then must be Fourier transformed in order to generate the magnitude and phase spectra. Zero degrees is arbitrarily determined by the spectrometer electronics but is reproducible for a given set of phase-modulation acquisition parameters. The acquired interferograms were transformed into non-negative single beam in-phase and quadrature spectra using the COMPUTE algorithm in the Win-IR Pro software with strong Norton–Beer apodization. From these single-beam spectrum pairs the magnitude spectra, M, were calculated using

$$M = (S_{IP}^2 + S_Q^2)^{1/2} \quad (2)$$

for both the 400 Hz and 25 Hz data, where S_{IP} and S_Q are the in-phase and quadrature component single-beam spectra, respectively.

The phase spectra, S_θ, were also calculated from the same single-beam spectrum pairs, using the equation

$$S_\theta = \arctan(S_Q/S_{IP}) \quad (3)$$

Since the COMPUTE algorithm yields non-negative single beam spectra, caution in interpreting the phase spectra using this approach must be exercised. Phase can become ambiguous because the computed phase spectrum is restricted to a single quadrant, 0° to 90°, when S_{IP} and S_Q are both positive. Signals whose true phase is outside this quadrant will usually be folded back into the quadrant appearing at false angles, somewhat akin to aliasing in Fourier transforming.[29] When this occurs, the initially calculated points of S_θ must therefore be unfolded back into their true quadrant when the 0° or 90° boundary is crossed. (It should be noted that the Mertz correction, which is universally instituted in FT-IR spectrometers, is a low resolution phase rotation designed to compensate for the variation in instrumental phase with wavelength so that all spectrum points are positive valued. The rapid (high resolution) and sometimes large phase shifts observed in our photoacoustic spectra can be more than the Mertz correction can handle, so some points in S_{IP} and S_Q can be negative, resulting in phase points outside the 0° and 90° quadrant via Eq. 3.)

An example of the ambiguity that arises when the phase is forced into the 0° to 90° quadrant is illustrated by applying Eq. 3 to the non-negative 400 Hz phase modulation single-beam data set. The phase spectra that are generated yield photoacoustic phase values that are larger in the high absorption coefficient regions than those in the low absorption coefficient regions as shown in the phase spectrum in Fig. 1 (uncorrected in-phase spectrum). However, according to previous work and theory,[15,30,31] the photoacoustic phase should shift to earlier (i.e., smaller) phase values as the absorption coefficient increases. This indicates that the computed phase spectra for the 400 Hz data set does not lie in the 0° to 90° quadrant. To ascertain which quadrant the 400 Hz data set should be in and what the proper phase values should be, the approach outlined by Jones and McClelland[3] was used. This approach uses the orthogonal interferogram pair, I_0 and I_{90}, to determine the phase spectrum and places the phase between 0° and 180°. By using this approach, it was determined that the photoacoustic phase of the 400 Hz set should lie in the 90° and 180° quadrant, meaning that the true in-phase spectrum, S_{IP}, is actually negative valued. Therefore, S_{IP} produced by the basic Fourier transform must be negated prior to using Eq. 3. The result of negating S_{IP} for a particular single-beam pair is shown in Fig. 1 (negated in-phase spectrum). Negating S_{IP} re-

† Calculated from physical properties of Apiezon grease obtained from technical data sheet, Apiezon Products, M&I Materials Ltd, Manchester, UK.

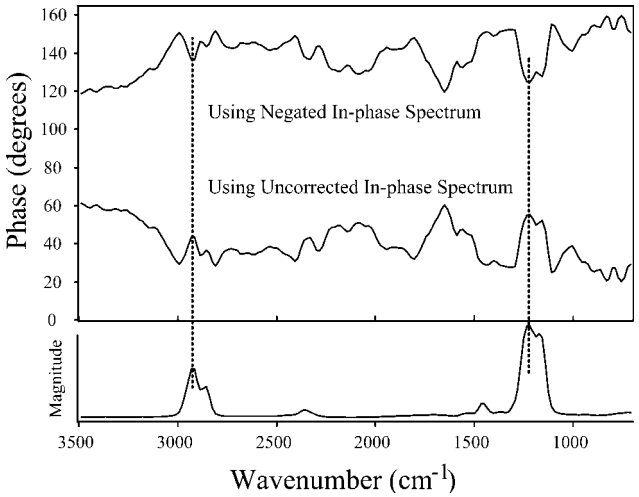

FIG. 1. Phase spectra generated from the same in-phase and quadrature single-beam pair taken at 400 Hz phase modulation. The top phase spectrum was generated after the in-phase single beam was negated. A normalized magnitude spectrum is included to denote regions of strong absorptions, which are indicated by dotted vertical lines. (Note: Zero degrees is arbitrarily determined by the spectrometer electronics but is reproducible for a given set of phase modulation acquisition parameters.)

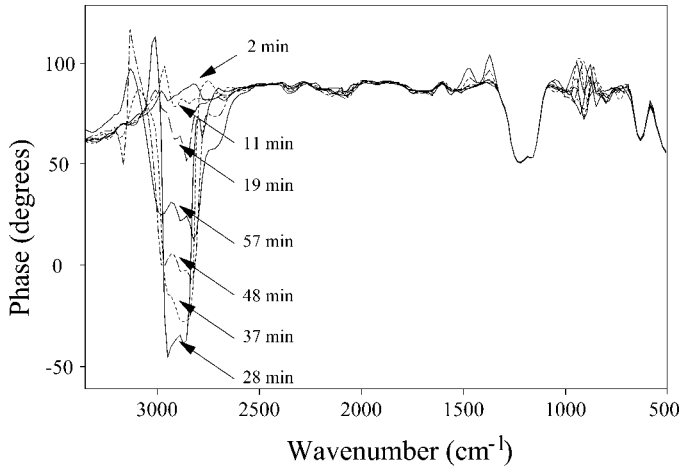

FIG. 2. Phase spectra for the first seven acquisitions from the 25 Hz phase modulation data set generated from Eq. 3. Times indicate when data acquisition was initiated after diffusion started.

sults in a phase spectrum with its strongly absorbing features pointing toward faster phase values and the phase spectrum properly placed in the 90° to 180° quadrant. A normalized magnitude spectrum is included at the bottom of the figure to identify strong absorption regions, which are identified by dotted vertical lines. The features near 1650 cm^{-1}, 2100 cm^{-1}, and 3500 cm^{-1}, although exhibiting relatively fast phases, correspond to regions where the grease/Teflon system absorbs little. A possible explanation for these features is the background signal from the photoacoustic chamber. A thin oxide layer on a high thermal conductivity metal surface, such as the chamber wall, generates a fast phase signal[30] that becomes a factor in spectral regions where the sample absorbance is low. Applying the same tests to the 25 Hz phase modulation data set showed that the true phase of the Teflon spectra fell between 0° and 90°, so no prior processing of the single beam spectra was required.

Further complications arise when the phases of individual absorption bands are in different phase quadrants from the rest of the spectrum. Such is often the case for the strong CH stretch absorption bands we observed from the grease layer. The phases of the CH absorption bands are directly related to the lag that the thermal wave, which is generated in the grease, experiences as it travels through the layer of ungreased Teflon film. Light penetration into the greaseless Teflon film is expected to be quite deep in the areas where the grease absorbs, since the absorption coefficients of Teflon are very small in these regions. Furthermore, since the thermal wave decay process is exponential, photoacoustic signal contributions will come from more than one thermal diffusion length into the Teflon.[32] Consequently, large photoacoustic phase values are expected early in the diffusion process. The grease steadily moves toward the surface of the Teflon during the diffusion. The photoacoustic phase of the CH absorption bands, accordingly, should steadily shift toward smaller values as the grease gets closer to the surface of the Teflon film. The shift toward smaller values results from the fact that as the grease moves toward the surface, the overlying greaseless Teflon film thickness gets smaller and the thermal wave experiences less of a lag. This shift should be reflected in the phase-time evolution curve as a smooth, constantly changing curve, but the forcing of phase by the software into a single quadrant complicates the observed behavior.

Figure 2 shows the computed phase spectra for the first seven time points of the 25 Hz phase-modulation data set generated from Eq. 3. The figure illustrates how the absorption coefficient affects the photoacoustic phase. Features that are pointing down (toward smaller phase values) correspond to regions (grease and Teflon absorption bands) with large absorption coefficients. The first three points in the 25 Hz data set (taken at 2, 11, and 19 minutes) show that as the diffusion progresses the photoacoustic phase of the strong CH absorption band from the grease layer (centered at 2920 cm^{-1}) shifts toward smaller values. The fourth data point (taken at 28 minutes), however, shows a rather abrupt phase shift to a large negative value for the strong CH absorption band. The following phase values (data points at 37, 48, and 57 minutes) now indicate that the trend of the photoacoustic phase has reversed and is shifting toward larger phase values (i.e., smaller negative numbers).

This reversal can be better observed in a plot of photoacoustic phase as a function of time. Figure 3a shows the raw data for the time evolution of the photoacoustic phase for the strong CH absorption band from the grease. Two photoacoustic phase trend changes or reversals are observed. These reversals are examples of the photoacoustic phase folding back into a single quadrant. One fold occurs at 28 minutes, as mentioned above, and the other at 74 minutes (9th data point). These folds reflect the fact that the photoacoustic phase in the region where the strong CH absorption band absorbs is passing from one quadrant to another as the diffusion progresses.

Working from later times in the diffusion to earlier times one can determine from which quadrant the photoacoustic phase of the CH absorption band from the

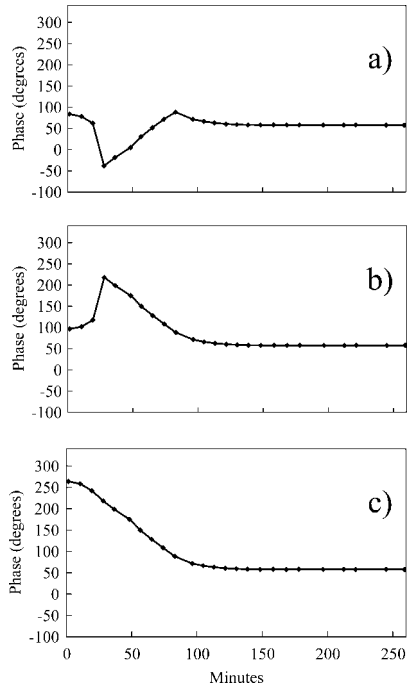

FIG. 3. Photoacoustic phase (25 Hz phase modulation frequency) versus time evolution curves of the strong CH absorption band from the grease layer. (**a**) Raw phase values extracted from phase spectra generated from Eq. 3. (**b**) Corrected phase values reflecting photoacoustic phase passing from the 90° to 180° quadrant into the 0° to 90° quadrant after the ninth point. (**c**) Corrected phase values reflecting photoacoustic phase passing from the 180° to 270° quadrant into the 90° to 180° quadrant after the third point.

grease is transitioning. At the end of the diffusion, the CH absorption band phase is near 60° and in the same quadrant as the rest of the spectrum. Moving toward earlier times, we see the photoacoustic phase values gradually increase toward 100°, whereupon the phase trend abruptly changes (at 74 minutes) and starts to decrease in value. This indicates that the photoacoustic phase at this point in the diffusion processes is passing from the 90° to 180° quadrant before 74 minutes into the 0° to 90° quadrant after that. From trigonometry, the proper phase values for the data at earlier times due to the quadrant change can be corrected by

$$180° - \theta_{computed} = \theta_{c(1)} \quad (4)$$

where $\theta_{computed}$ is the computed phase value from Eq. 3 at 2920 cm^{-1} and $\theta_{c(1)}$ is the corrected phase value reflecting the first quadrant change. Figure 3b shows the phase-time evolution curve after the phase corrections were made to the earlier data. The photoacoustic phase values for the first nine data points now lie in the 90° to 180° quadrant. Continuing to work from later times to earlier, another change in the phase trend is observed at the fourth data point. This point indicates that the photoacoustic phase is traversing yet another quadrant boundary as it passes from the 180° to 270° quadrant into the 90° to 180° quadrant. Again from trigonometry, the proper phase values for the first three data points due to this quadrant change were assigned by

$$180° + \theta_{c(1)} = \theta_{c(2)} \quad (5)$$

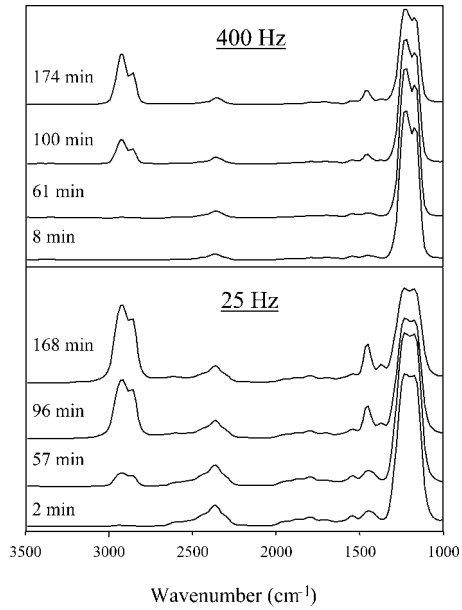

FIG. 4. Normalized magnitude spectra of Teflon and Apiezon-L taken at different times during the diffusion experiment at the two different modulation frequencies. The spectra in each panel are on the same ordinate scale but offset for clarity.

where $\theta_{c(2)}$ is the corrected phase value reflecting the second quadrant change.

Figure 3c shows the photoacoustic phase as a function of time after corrections were made to account for the quadrant changes. The corrected phase data for the 25 Hz phase modulation data set now shows that the photoacoustic phase for this absorption band actually starts out at a phase value of approximately 260° and gradually shifts toward smaller phase values until it levels off at approximately 60° at the end of the diffusion, passing through three quadrants during the duration of the experiment. A similar quadrant correction needed to be performed for the 400 Hz phase modulation data set for the CH absorption band of the grease layer, which passes through two quadrants. No quadrant changing corrections were needed for the observed phases of the other monitored absorption bands for either data set.

DISCUSSION

Data for the diffusion process were taken sequentially, alternating between the two modulation frequencies. Figure 4 shows typical normalized magnitude spectra acquired at different times during the experiment for each modulation frequency and illustrates the absorption bands used to monitor the diffusion process. The spectra in each panel are on the same ordinate scale but offset for clarity. Apiezon-L, which has an infrared absorption spectrum similar to that of polyethylene, has a strong C–H stretch at 2920 cm^{-1} and a weaker C–H bend at 1450 cm^{-1}. The strong C–F absorption band at 1230 cm^{-1} was used to monitor the Teflon film during the experiment. Teflon also has a weak absorption band at approximately 2360 cm^{-1}, which was not used because of its proximity to carbon dioxide absorption bands (approximately 2350 cm^{-1}).

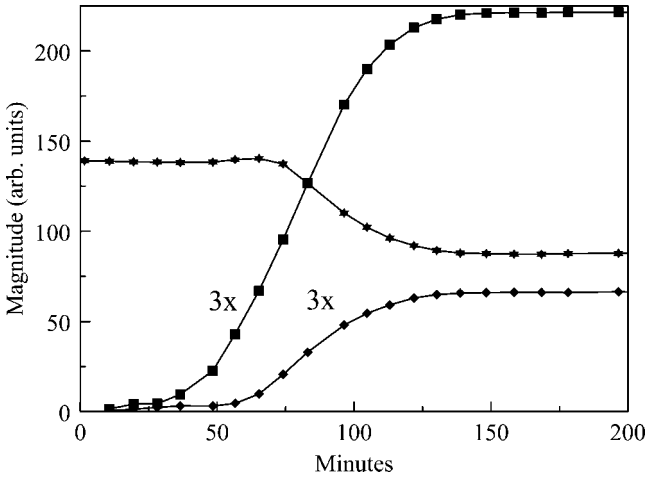

FIG. 5. Magnitude versus time evolution curve for all monitored bands at 25 Hz phase modulation. Grease bands are isolated from Teflon signal contribution. The magnitudes of the grease bands have been multiplied by a factor of 3 for scaling. (–■– = strong CH absorption band (2920 cm^{-1}); –◆– = weak CH absorption band (1450 cm^{-1}); –★– = Teflon band (1230 cm^{-1}).)

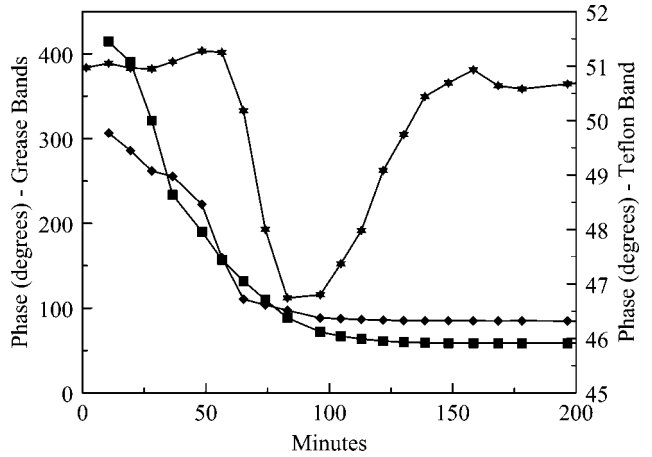

FIG. 6. Phase versus time evolution curve for all monitored bands at 25 Hz phase modulation. Grease bands are isolated from Teflon signal contribution. Teflon and grease bands are plotted on different ordinate scales. (–■– = strong CH absorption band (2920 cm^{-1}); –◆– = weak CH absorption band (1450 cm^{-1}); –★– = Teflon band (1230 cm^{-1}).)

The figure further illustrates that the lower modulation frequency samples deeper into the Teflon film than the higher modulation frequency, as evidenced by the acquisitions taken at 57 and 61 minutes, which show that the strong CH absorption band at 2920 cm^{-1} is present in the 25 Hz phase-modulation magnitude spectrum and is absent in the 400 Hz phase-modulation magnitude spectrum. Note also that as the diffusion progresses the magnitude of the Teflon absorption band changes (decreases) for both modulation frequencies.

It is important to recognize that during the earlier stages of the diffusion when the grease absorptions are weak, the major signal contribution is a background signal from the cell and the Teflon film. This background signal contribution will lead to erroneous interpretation of the phase data if it is not taken into account. Since we are interested solely in monitoring the progress of the grease through the Teflon, all of the phase and magnitude data collected were ''corrected'' to isolate the grease signal from that of the Teflon and any other contributor to the total signal. This isolation process has been described by Jones and McClelland.[3] The isolation involves realizing that the total observed magnitude and phase at a given wavenumber is actually the vector sum of the overlapping grease and Teflon/background contributions. To obtain the magnitude and phase of the Teflon film and any background contributions, it was assumed that the first measurement at each modulation frequency was only of the film and any background contribution, with none of the grease present. Once the magnitude and phase of the Teflon and background were determined, they were geometrically subtracted out from the rest of the respective data set by using the following equations:

$$M_{\text{Grease}} = [M^2_{\text{Total}} + M^2_{\text{Tef}} - 2M_{\text{Total}}M_{\text{Tef}}\cos(\theta_{\text{Total}} - \theta_{\text{Tef}})]^{1/2} \quad (6)$$

If $\theta_{\text{Total}} > \theta_{\text{Grease}}$, then

$$\theta_{\text{Grease}} = \theta_{\text{Total}} - \cos^{-1}\left(\frac{M^2_{\text{Total}} + M^2_{\text{Grease}} - M^2_{\text{Tef}}}{2M_{\text{Total}}M_{\text{Grease}}}\right) \quad (7)$$

and if $\theta_{\text{Total}} < \theta_{\text{Grease}}$, then

$$\theta_{\text{Grease}} = \theta_{\text{Total}} + \cos^{-1}\left(\frac{M^2_{\text{Total}} + M^2_{\text{Grease}} - M^2_{\text{Tef}}}{2M_{\text{Total}}M_{\text{Grease}}}\right) \quad (8)$$

where θ_{Total} and M_{Total} are the observed phase and magnitude, θ_{Grease} is the phase of the grease, θ_{Tef} is the phase of the Teflon and background, M_{Grease} is the magnitude of the grease, and M_{Tef} is the magnitude of the Teflon and background.

Figure 5 shows the magnitude of the isolated grease bands and Teflon band as a function of time at a phase modulation frequency of 25 Hz. The advance of the grease front is first observed at approximately 25 minutes as evidenced by the gradual increase in magnitude of both grease absorption bands. The magnitude of the Teflon absorption band remains constant till about 60 minutes into the process, when it begins to decrease. At about 50 minutes the magnitude of the grease absorption bands begins to rapidly increase, indicating that the grease is moving/diffusing toward the Teflon surface. The diffusion of the grease appears to end at approximately 160 minutes into the process when the magnitudes of all three absorption bands level off. The magnitude of the Teflon band decreases by about 35%. This decrease roughly corresponds to the percent pore volume of the clean Teflon film. The decrease follows from an increase in the heat capacity of the Teflon as the pores are filled with grease, effecting a decrease in temperature oscillation and photoacoustic signal magnitude.

Figure 6 shows the isolated phase of the grease bands as well as that of the Teflon absorption band for a phase modulation of 25 Hz. The grease and Teflon data are plotted on different ordinate scales for clarity. The phase of both grease bands are observed to be changing from the very beginning of the process, indicating that the phase measurements are much more sensitive than magnitude measurements in detecting the onset of diffusion. The greater sensitivity of the phase measurement is illus-

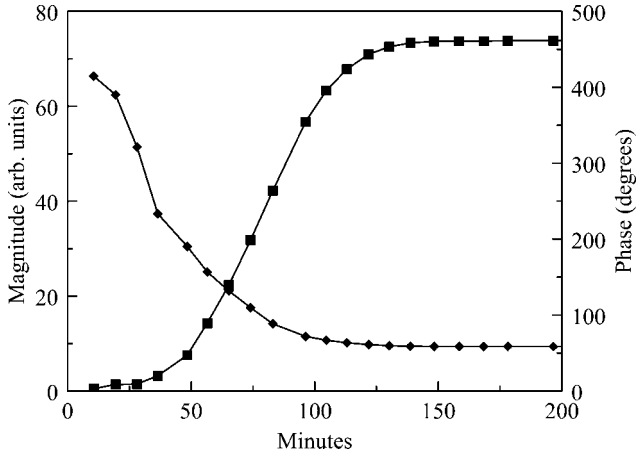

FIG. 7. Phase and magnitude of strong isolated CH absorption band from the grease layer at 25 Hz phase modulation frequency. (–■– = magnitude; –♦– = phase.)

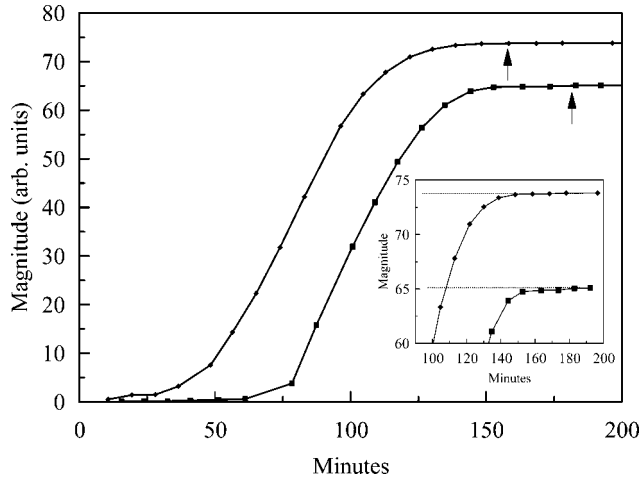

FIG. 8. Comparison of magnitudes for strong isolated CH absorption band from the grease layer at both modulation frequencies. The inset shows an expansion of magnitude–time curves at a late stage of diffusion. The arrows indicate the times when magnitude changes are no longer observed. (–■– = 400 Hz phase modulation; –♦– = 25 Hz phase modulation frequency.)

trated better in Fig. 7, which has the isolated phase and magnitude spectra of the strong CH absorption band overlaid. Interestingly, the photoacoustic phase for both grease bands shows very large shifts over the course of the diffusion experiment. For the strong grease band, the first phase value is at 415° and at the end of the diffusion process the phase value steadies out at 59°, which corresponds to a photoacoustic phase change of 356°. For homogeneous static samples, phase changes are expected to be within a 45° range, depending on the absorption coefficient. The large observed phase shifts are the result of infrared light penetrating deep into the Teflon substrate because of the low absorption coefficients of Teflon in regions where the grease absorbs and sampling depths greater than one thermal diffusion length contributing to the photoacoustic signal in spite of the exponential decay of the thermal wave. This phase change then can be used to estimate the distance of the grease front from the surface of the Teflon film by using the formula[6]

$$d = \Delta\theta L \tag{9}$$

where d is the distance of the grease front from the surface, $\Delta\theta$ is the difference in phase angle at a particular time in the diffusion process from the final phase angle, and L is the thermal diffusion length. From Eq. 9 the grease front is calculated to be approximately 224 μm from the surface of the film at the beginning of the process, which nearly equals the thickness of the Teflon film (approximately 254 μm) and roughly corresponds to six thermal diffusion lengths at a phase modulation frequency of 25 Hz.

Note that the phase of the Teflon absorption band at 1230 cm^{-1} also changes slightly during the diffusion process, going from 51° to 50° approximately after going through a minimum at 46.5°. During the diffusion process, the sample starts as a single-layer (pure Teflon) sample, transitions to a dynamic two-layer sample during the diffusion, and returns to a single-layer (two component Teflon/grease) sample after the diffusion is complete. As the grease begins moving into the film, the pores of the Teflon film become filled. Filling of the pores produces a layer of pure Teflon that physically is becoming thinner and thinner as the diffusion proceeds, resulting in the average phase becoming faster, since the majority of the signal at 1230 cm^{-1} is from the thinning layer, as evidenced by the observed dip in phase in Fig. 7. As the sample returns again to more like a single-layer type sample toward the end of the process, the phase returns to near its original value but slightly faster. This slight phase change arises from the change in the thermal diffusivity as the pure Teflon film becomes a two-component sample ($D_{\text{Teflon(solid)}} \leq D_{\text{Apiezon-L}}$).

A comparison of the increase of the strong CH absorption band at 2920 cm^{-1} over time at the two different phase modulation frequencies is shown in Fig. 8. As expected, the deeper probing 25 Hz phase modulation frequency measurement picks up the movement of the grease earlier (at approximately 25 minutes) in the diffusion process than the shallower 400 Hz measurement (approximately 50 minutes). The magnitude then rapidly increases for both phase modulation measurements as the grease fills empty pores and moves toward the surface. The magnitude no longer changes for the 25 Hz phase modulation frequency measurement at approximately the 160 minute mark of the process and at the 180 minute mark for the 400 Hz phase modulation measurement, as indicated by the arrows in Fig. 8.

The time evolution of the photoacoustic signal phase of the strong isolated CH absorption band from the grease layer is shown in Fig. 9 for both phase modulation frequencies. The data sets are plotted on different ordinates because phase values are not identical at the two different modulation frequencies (i.e., in terms of sample depth, a 1° change at 25 Hz corresponds to an approximately 4° change at 400 Hz). Phase changes for both modulation frequencies are observed from the beginning of the diffusion process. Data for the 400 Hz phase modulation measurement prior to 70 minutes are not shown because of the higher noise levels at early times when there is little grease signal. This (unplotted) data does however follow a comparable trend as the 25 Hz phase modulation measurement. The error associated with each observed phase value is depicted by the vertical lines. The phases

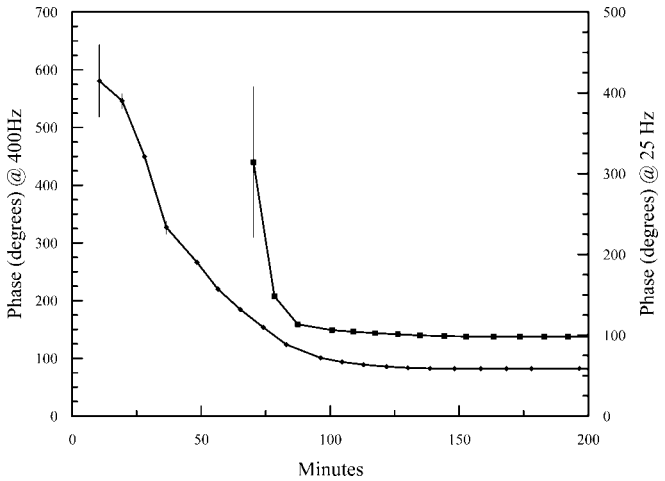

FIG. 9. Comparison of phase for the strong isolated CH absorption band from the grease layer at both modulation frequencies. Vertical lines on points represent estimated error. (–■– = 400 Hz phase modulation; –◆– = 25 Hz phase modulation frequency.)

shift toward smaller values indicating that the layer of ungreased Teflon film is becoming smaller as the grease moves toward the surface. The phase for both modulation frequencies appears to stop changing at approximately the 150 minute mark of the process, indicating that the grease front is sufficiently close to the surface that the phase is no longer affected. (Later stages of diffusion are better observed by photoacoustic magnitude.) It is interesting to note that over the course of the experiment a large phase shift of approximately 197° is also measured for 400 Hz phase modulation frequency.

CONCLUSION

This study has shown that step-scan phase modulation photoacoustic spectroscopy can follow the time evolution of a dynamic system, such as the permeation of a hydrocarbon grease through a porous Teflon film. Early stages of the diffusion appear to be best observed by phase changes, whereas the late stages are best monitored by magnitude changes. (Phase data prior to 70 minutes for 400 Hz phase modulation are not plotted due to high noise levels.) Diffusion induced changes for the 2920 cm^{-1} strong CH absorption band are observed in the phase of the photoacoustic signal within minutes (or less) after diffusion is initiated for both 25 Hz and 400 Hz phase modulation frequencies. These phase changes cease after approximately 150 minutes. Furthermore, magnitude changes are also observed for the strong grease band at approximately 25 minutes for 25 Hz phase modulation frequency and at approximately 50 minutes for 400 Hz phase modulation frequency after diffusion is initiated. Phase changes of approximately 197° and 356° are observed for the strong CH absorption band at 400 Hz and 25 Hz phase modulation frequencies, respectively, indicating sampling depths greater than one thermal diffusion length.

Magnitude and phase changes are also observed for the Teflon band during the diffusion process. An observed magnitude reduction of approximately 35% may be due primarily to an increase of the heat capacity as pores are filled with grease. The small observed increase in photoacoustic phase may be due to a change in the sample's thermal diffusivity.

ACKNOWLEDGMENTS

Ames Laboratory is operated by the U.S. Department of Energy by Iowa State University under Contract No. W-7405-ENG-82. This work was supported in part by the U.S. Department of Energy, Office of Science and Technology.

1. A. G. Bell, Am. J. Sci. **20,** 305 (1880).
2. S. J. Bajic, S. Luo, R. W. Jones, and J. F. McClelland, Appl. Spectrosc. **49,** 1000 (1995).
3. R. W. Jones and J. F. McClelland, Appl. Spectrosc. **50,** 1258 (1996).
4. L. Gonon, O. J. Vasseur, and J.-L. Gardette, Appl. Spectrosc. **53,** 157 (1999).
5. A. Beenen, G. Spanner, and R. Niessner, Appl. Spectrosc. **51,** 51 (1997).
6. M. J. Adams and G. F. Kirkbright, Analyst (Cambridge, U.K.) **102,** 281 (1977).
7. R. A. Palmer and R. M. Dittmar, Thin Solid Films **223,** 31 (1993).
8. E. Y. Jiang and R. A. Palmer, Anal. Chem. **69,** 1931 (1997).
9. R. M. Dittmar, J. L. Chao, and R. A. Palmer, Appl. Spectrosc. **45,** 1104 (1991).
10. Y. Kano, S. Akiyama, T. Kasemura, and S. Kobayashi, Polymer J. **27,** 339 (1995).
11. R. J. W. Hodgson, J. Appl. Phys. **76,** 7524 (1994).
12. C. Glorieux, J. Fivez, and J. Thoen, J. Appl. Phys. **73,** 684 (1993).
13. E. Y. Jiang, R. A. Palmer, and J. L. Chao, J. Appl. Phys. **78,** 460 (1995).
14. L. E. Jurdana, K. P. Ghiggino, I. H. Leaver, and P. Cole-Clark, Appl. Spectrosc. **49,** 361 (1995).
15. A. Rosencwaig and A. Gersho, J. Appl. Phys. **47,** 64 (1976).
16. D. L. Drapcho, R. Curbelo, E. Y. Jiang, R. A. Crocombe, and W. J. McCarthy, Appl. Spectrosc. **51,** 453 (1997).
17. V. G. Gregoriou and R. Hapanowicz, Spectroscopy **12(5),** 37 (1997).
18. J. F. McClelland, S. J. Bajic, R. W. Jones, and L. M. Seaverson, ''Photoacoustic Spectroscopy'', in *Modern Techniques in Applied Molecular Spectroscopy*, F. M. Mirabella, Ed. (John Wiley and Sons, New York, 1998), pp. 221–265.
19. Y. S. Tung, R. Mu, D. O. Henderson, and W. A. Curby, Appl. Spectrosc. **51,** 171 (1997).
20. S. Ekgasit and H. Ishida, Appl. Spectrosc. **51,** 461 (1997).
21. G. T. Fieldson and T. A. Barbari, Polymer **34,** 1146 (1993).
22. C. A. Gagliardi, L. B. Muire, and D. E. Hirt, *57th Annual Technical Conference—Society of Plastics Engineers* **2,** 2502 (1999).
23. O. Wattraint and C. Sarazin, Biochim. Biophys. Acta **1713,** 65 (2005).
24. A. Uenver, N. Dilsiz, M. Volkan, and G. Akovali, J. Appl. Polym. Sci. **96,** 1654 (2005).
25. S. H. Hosseini and A. A. Entezami, J. Appl. Polym. Sci. **90,** 1654 (2003).
26. S. Slomkowski, in *Modification and Blending of Synthetic and Natural Macromolecules, Vol. 175, NATO Science Series, II. Mathematics, Physics and Chemistry*, F. Ciardelli and S. Penczek, Eds. (Kluwer Academic Publishers, New York, 2004), p. 317.
27. R. O. Carter III, M. C. Paputa Peck, M. A. Samus, and P. C. Killgoar, Jr., Appl. Spectrosc. **43,** 1350 (1989).
28. D. R. Anderson and R. U. Acton, ''Thermal Properties'', in *Encyclopedia of Polymer Science and Technology*, H. F. Mark, N. G. Gaylord, and N. M. Bikales, Eds. (John Wiley and Sons, New York, 1970), vol. 13, p. 780.
29. P. R. Griffiths and J. A. de Haseth, *Fourier Transform Infrared Spectrometry* (John Wiley and Sons, New York, 1986), p. 527.
30. A. Mandelis, Y. C. Teng, and B. S. H. Royce, J. Appl. Phys. **50,** 7138 (1979).
31. Y. C. Teng and B. S. H. Royce, J. Opt. Soc. Am. **70,** 557 (1980).
32. J. F. McClelland, Anal. Chem. **55,** 89A (1983).